This is an accepted version of the article. The final version is available at:
https://doi.org/10.1016/j.polymertesting.2017.05.003

Elastic recovery after compression in HNBR at low and moderate temperatures: Experiment and modelling

Anton G. Akulichev[1*], Ben Alcock[2] and Andreas T. Echtermeyer[1]

[1] The Norwegian University of Science and Technology,
Department of Mechanical and Industrial Engineering ,
Richard Birkelands vei 2 B, 7034 Trondheim, Norway
[2]SINTEF Materials and Chemistry, Forskningsveien 1, 0373 Oslo, Norway
*Phone +47-958-24-097, Fax +47-73-59-41-29, e-mail: anton.akulichev@ntnu.no

Abstract

Elastic recovery after compression or compression set is one of the key indicators of elastomer performance in sealing applications, such as O-rings in flange joints. In this work, findings of a study of the compression set property of a hydrogenated nitrile butadiene rubber (HNBR) at temperatures above and below the glass transition temperature T_g are presented. The compression set in the elastomer is found to increase with cooling up to 100 % at the glass transition temperature and decrease with time after unloading even at temperatures below T_g. The effects of reinforcing filler (carbon black) and the initial compression time are also considered. Equivalence of time and temperature effects on the compression set of the elastomers is then demonstrated. A viscoelastic model describing the time-temperature variation of the compression set is proposed and verified by finite element analysis (FEA) and experimental results. It is shown that modelling captures well the experimental behaviour of the elastic recovery of the studied HNBR at ambient and low temperatures.

1. Introduction

Rubbers or elastomers typically exhibit high resilience properties which make these materials almost ideal candidates for pressure sealing applications. The excellent elastic recovery or low compression set enables the rubber seals to compensate for any movements of the sealed parts, e.g. the sealing gap growth caused by pressure peaks. However the sealing performance is often jeopardized by freezing conditions since rubbers become much less resilient at low temperatures near their glass transition point. This effect is schematically illustrated in Figure 1.

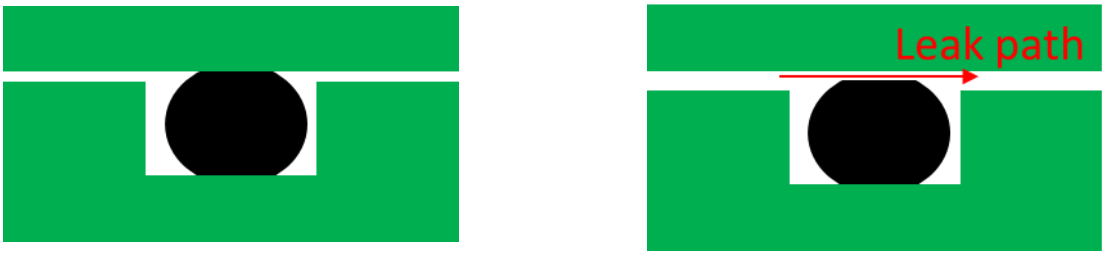

a) b)

Figure 1. Schematic of compressed O-ring seal (black) in a flange: a) at ambient temperature; b) upper part lift-off at low temperature and leakage due to “frozen” seal

In reality the contact of rubber seal and its counter surface might be much more complicated on different length scales including micrometer and sub-micrometer ranges [1]. Nevertheless even a sudden microscopic separation can promote leakage if the seal material exhibits no or negligible elastic recovery as depicted in Figure 2. Therefore understanding the effect of cold environments on the recovery properties of elastomer compounds is of high interest for a number of branches of industry which use machinery operated under high pressure and exposed to low temperatures.

a) b)

Figure 2. Schematic magnified view of rubber seal surface (black) in contact with a rigid counter surface: a) at ambient temperature; b) rigid surface lift-off and leakage at low temperatures

Despite its importance in many practical applications, the elastic recovery or set properties at low temperatures are covered rather scarcely in academic literature. Morris et al [2] reported high compression set values for several rubber systems exposed to cold environment and noticed that the set effect is reversible upon warming to the ambient temperature. Similar effects of low temperatures on the elastic recovery in styrene butadiene rubber (SBR) and nitrile butadiene rubber (NBR) were later described in [3]. The same authors reported the effect of crystallization in natural rubber (NR) on the elastic recovery [4]. Baranov and Elkin [5] investigated the development of the elastic recovery and the contact area of elastomeric ring seals with gradual temperature reduction down to -70 °C. They found the recovery was uneven along the contact width of the compressed seals and it was also stress dependent. Bukhina and Parizenberg [6] applied the time temperature superposition (TTS) principle to the rubber recovery at different temperatures and constructed the recovery master curves for several compounds. Jaunich et al [7, 8] recently investigated low-temperature recovery of various rubber compounds by a modified compression set method using a dynamic mechanical analysis (DMA) machine and demonstrated effects of temperature, elastomer nature, the degree of compression, and the machine contact pressure on the compression set development over time.

Summing up the available publications, there exists very few reports and experimental studies of the cold recovery of elastomers and particularly no data on hydrogenated nitrile butadiene rubber (HNBR) was found even though this material is of great importance for the oil and gas industry. The main objectives of this work are therefore to study the low-temperature strain recovery property of a model HNBR compound and to elucidate the effect of carbon black as a reinforcing filler on this property. In addition, the recovery behaviour at various temperatures is modelled based on the established mathematical concepts for viscoelastic materials.

2. Materials and experimental procedure

2.1 Materials and processing

A typical rubber formulation widely used in seals in the oil and gas industry was tested. The composition is based on hydrogenated nitrile butadiene rubber with 96 % saturated polybutadiene with 36 % acrylonitrile content and varied carbon black (CB) content from 0 to 50 phr (parts per hundred rubber). For ease of description, the formulation without carbon black is hereafter referred to as "unfilled" HNBR, while the formulation contained 50 phr carbon black is referred to as "filled" HNBR. The compound formulae are detailed in Table 1.

Table 1 Composition of the generic HNBR used in this study

Component	Content, phr
HNBR	100
Antioxidant	3
Stearic acid	0.5
Zinc oxide	5
Magnesium oxide	10
Plasticizer	20
Peroxide	10
N-330 HAF carbon black	0 or 50

The compounds (except the peroxide) were combined in an internal mixer to yield a single HNBR masterbatch which was then mixed with the peroxide in a two roll mill. Compression moulding and vulcanization in a press at 170 °C for 20 min followed. Finally, a post-curing operation at 150 °C for 4 h in an oven was carried out. More information about the processing and the basic material test data is available in our previous publication [9]. The vulcanised unfilled HNBR has Shore A hardness of 70±5, while the carbon black filled material has Shore A hardness of 85±5.

2.2 Test methods

2.2.1 Dynamic mechanical thermal analysis

Dynamic mechanical thermal analysis (DMTA) was carried out on an Eplexor 150 DMTA machine equipped with a 150 N load cell and a thermal chamber. A temperature sweep was performed using the tension loading mode and the testing frequency of 1 Hz. Specimens for the experiments were

nominally 8 mm wide and 2 mm thick moulded-to-shape bars. The temperature was swept in the range of -60 to 120 °C. For each temperature step, the specimens were pre-loaded to 0.05 % of the initial length on top of which a cycling strain with the amplitude of 0.02 % was applied. The specimen was unloaded each time before moving to a new temperature step to reflect changes in the specimen length.

2.2.2 Compression strain recovery

At least 2 standardised methodological approaches to measure elastic recovery of rubber materials in compression at low temperatures exist. The first method is based on compression set (CS) measurements and described in ISO 815-2 [10], while the other is called elastic rebound after compression and implemented in Russian GOST 13808-79 [11]. The principal formulae for calculation of the recovery parameters and the essential testing conditions are summarized in Table 2.

Table 2. Comparison between ISO 815-2 and GOST 13808-79

Test conditions	ISO 815-2	GOST 13808-79
Initial compression	25 % for hardnesses below 80 IHRD 15 % for hardnesses between 80-89 IHRD 10 % for hardnesses above 90 IHRD	20 ± 2 %
Specimen geometry	A: Ø 29 x 12.5 mm B: Ø 13 x 6.3 mm	Ø 10 x 10 mm
Test duration (cold exposure)	24 or 72 hours	5 min
Specimen recovery time	30 ± 3 min	3 min
Principal equation	$CS = \frac{h_0 - h(t)}{h_0 - h_c}$	$K_r = \frac{h(t) - h_c}{h_0 - h_c}$
The principal equation in terms of engineering strain	$CS = \frac{\varepsilon(t)}{\varepsilon_0}$	$K_r = 1 - \frac{\varepsilon(t)}{\varepsilon_0}$
Here *CS* is the compression set parameter; K_r is the coefficient of elastic recovery; h_0 is the initial thickness of the specimen; $h(t)$ is the thickness after recovery time t; h_c is the compressed thickness of the specimen. $\varepsilon_0 = \frac{\Delta h}{h_0} = \frac{h_0 - h_c}{h_0}$ is the initial compressive strain; $\varepsilon(t) = \frac{h_0 - h(t)}{h_0}$ is the strain after recovery time t.		

The compression set approach was followed in this study. Nevertheless, as it is immediately deduced from the equations, these two recovery metrics are related if we assume equal testing conditions (i.e. specimen geometry, initial compression, duration of the experiment and the elapsed time t at the property measurement).

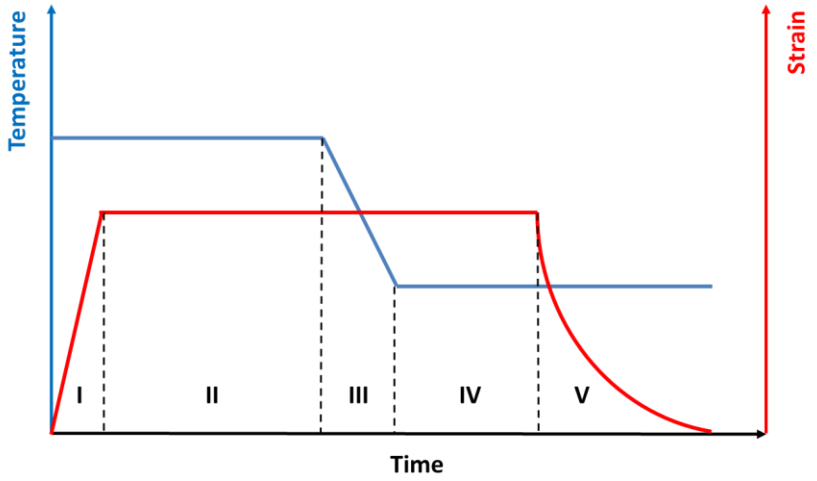

Figure 3. Schematic of the low-temperature strain recovery test procedure: I – loading step; II – stress relaxation step; III – cooling (heating) step; IV – temperature conditioning period; V – recovery step (load released)

The strain recovery tests were carried out using the same Eplexor 150 DMTA machine using a 1500 N load cell and parallel plate compression holders. The specimens were cylindrical with 10 mm nominal diameter and 6 mm height. The testing procedure in this work was somewhat different with the major change being the duration of the holding time under the freezing conditions which was set to 30 min as compared to 24 hours in the ISO standard. The procedure illustrated in Figure 3 was automatized in the machine. First a rubber specimen was compressed to 85% of its initial height (step I) and left to relax at room temperature for 6 hours (step II). This is to reflect the practical application in which rubber seals are rarely pressurized or exposed to the service environment immediately after installation. Nevertheless the impact of the duration of the compression step was also included into the investigation. After the compression step, the rubber specimen was exposed to the required temperature and held under load over 30 min (steps III and IV). Then the compression load was quickly removed keeping, however, 2 N compressive force in order to maintain the contact with the specimen. The specimen height change was recorded over time starting from the point of unloading (step V). The compression set values reported hereafter correspond to the time of 30 min after unloading (as in ISO 815-2) unless stated otherwise or designated by the time.

3. Results

3.1 Dynamic mechanical thermal analysis

Figure 4 depicts the outcome of DMTA for both HNBR compounds (i.e. unfilled and filled with 50 phr carbon black). As expected, the addition of carbon black results in a significant increase of the dynamic moduli [12, 13]. In contrast with the material stiffness, the filler does not produce a noticeable impact on the glass transition temperature which is determined from the tan delta peak maximum to be about -16 °C for 1 Hz testing frequency in both cases.

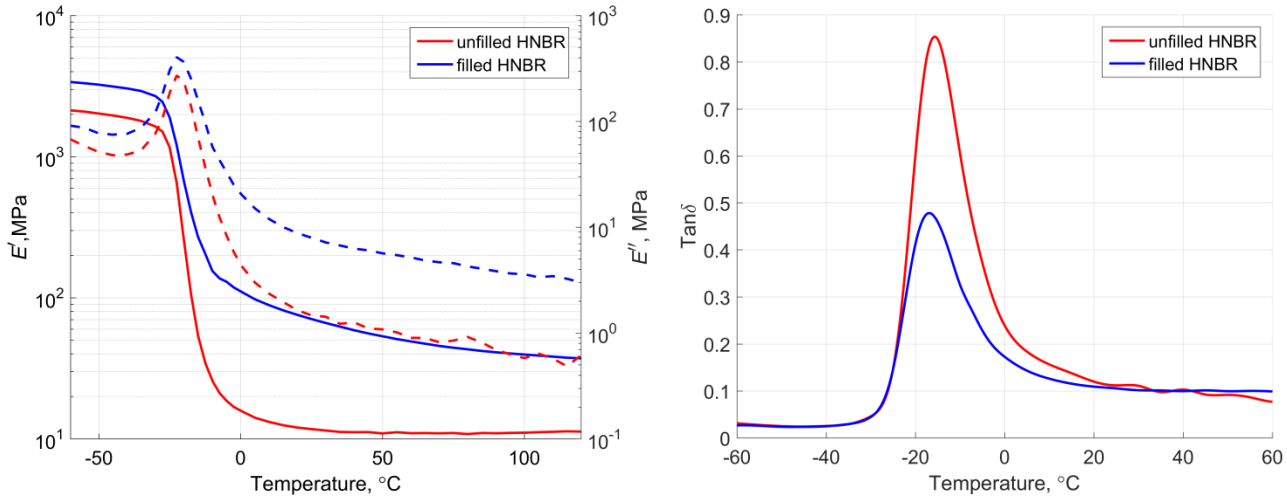

a) b)

Figure 4. DMTA testing results taken at 1 Hz frequency:

a) Storage (solid line) and loss (dashed line) moduli as a function of temperature;

b) Tan delta as a function of temperature. Spline interpolated data.

3.2 Strain recovery and compression set

Preliminary compression set (CS) experiments in a freezing cabinet indicate that the studied HNBR demonstrates almost no elastic recovery already at -25 °C, only a few degrees below T_g. Moreover, if the elastomer is sufficiently compressed against a rough surface, such as sand paper in Figure 5, the counter-surface topography is mirrored on the elastomer specimen surface after unloading in a freezing environment. The observed set is not permanent. As already noticed by Morris et al [2], putting the cold CS specimens back to the ambient condition leads to relatively quick (10-20 min) restoration of the major portion of their original shapes.

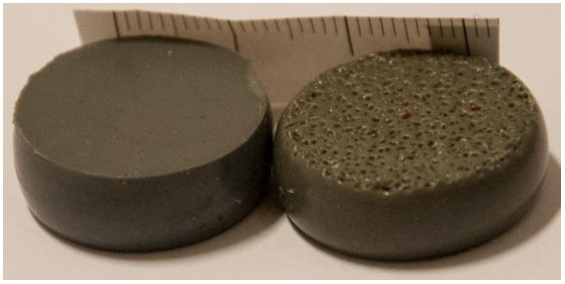

Figure 5. Unfilled HNBR CS specimens photographed 3 min after load release at -25 °C. 20 % nominal compression was imposed, and the specimen on the right was compressed against sandpaper (photo courtesy of Natalia Akulicheva). The scale bar behind the specimens indicates mm.

More quantitative CS experiments at various temperatures down to -30 °C followed. The processed strain recovery data is plotted in Figure 6 as a variation of compression set with time and temperature for both studied HNBR compounds. The compression set is seen to increase with cooling below the ambient temperature, and it rises steeply near the glass transition point. This is in line with the previous observations in other elastomers [3, 4, 6-8]. At the temperature of -30 °C,

both compounds lose their resilience completely and do not regain their undeformed shapes as demonstrated by their compression set values of 95-100% at the short times. As expected, the compression set in HNBR has also a strong time-dependent nature. It gradually decreases as the recovery time progresses at all temperatures. Even at the lowest temperature some recovery is evident but it occurs at a very slow rate.

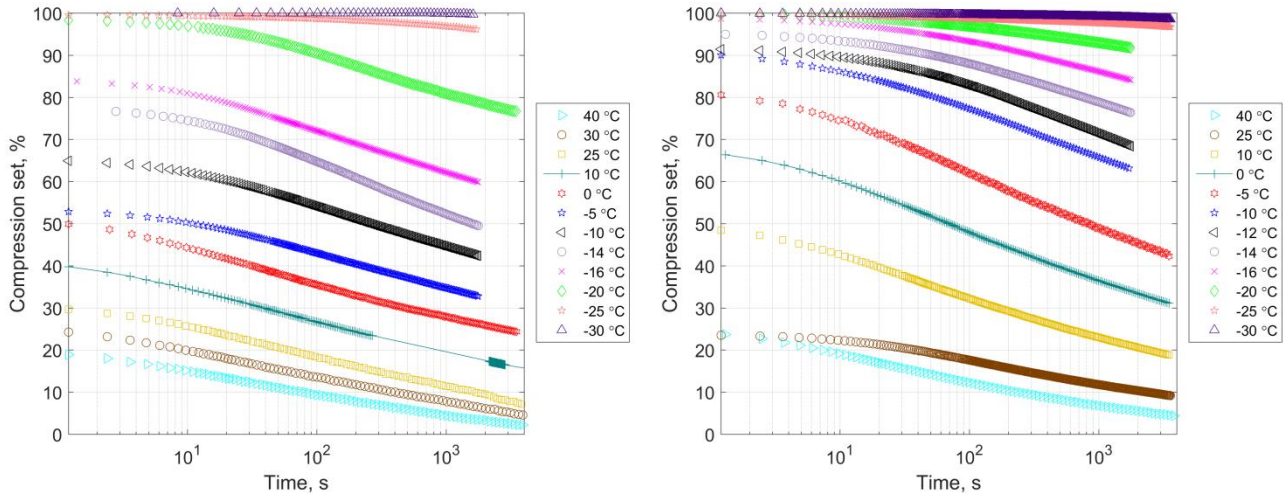

a) unfilled HNBR b) 50 phr CB filled HNBR

Figure 6. Compression set as a function of time at the indicated temperatures

It is noteworthy that the filled HNBR has inferior compression set characteristics at sub-ambient temperatures above the glass transition point if compared to the unfilled HNBR, even though they exhibit close magnitudes of compression set at room and elevated temperatures. This result is in good agreement with the CS measurements carried out using zirconium tungstate filled HNBR [9] where a noticeable increase of CS in the filled rubber was also observed. The difference in CS between the carbon black filled and the virgin compound enlarges with temperature reduction peaking near the T_g region, which is seen in Figure 6 and more clearly in Figure 7.

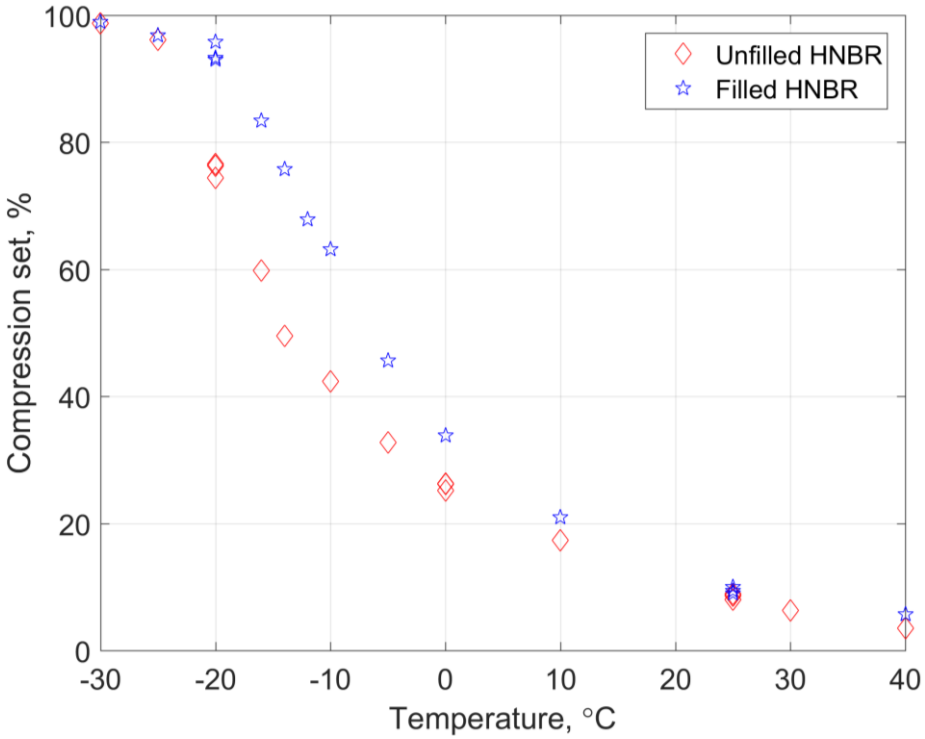

Figure 7. Compression set as a function of temperature (30 min after unloading)

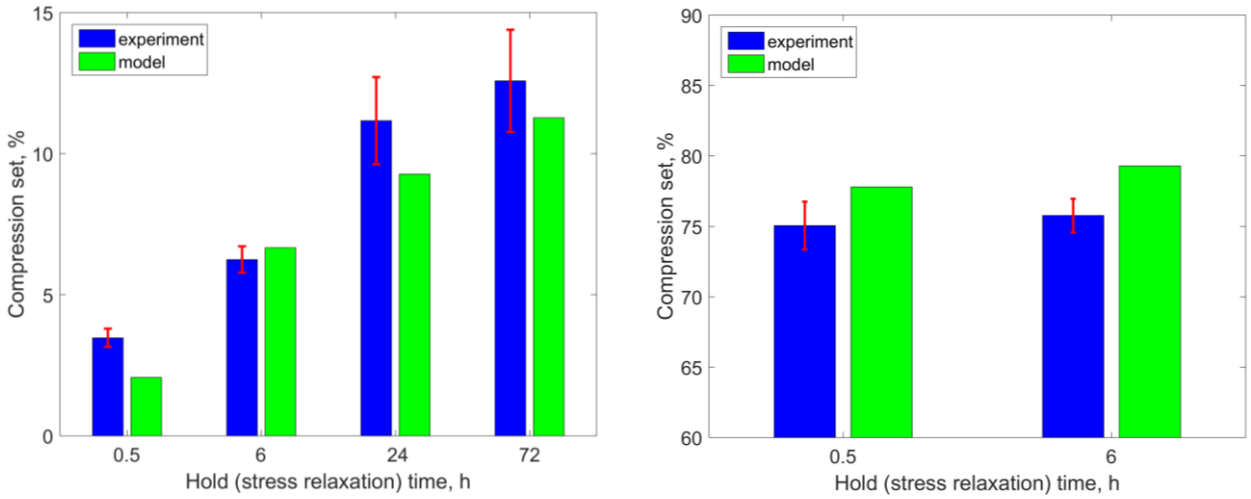

a) b)

Figure 8. Effect of the hold time (step II) at room temperature on the compression set of the unfilled HNBR: a) at room temperature and b) at -20 °C. The error bars indicate the standard deviation. The data for 24 and 72 hours hold time are taken from the previous study [9]. The modelling approach and the predictions are to be described in sections 4.1 and 4.3.

Figure 8 demonstrates how the initial compression time at room temperature influences the compression set property at room temperature and at T_g. The room temperature CS clearly increases with the duration of the initial squeeze, while the results at T_g show no considerable effect of the compression time on the recovery of HNBR. Therefore keeping the CS specimens over a long time interval under compression at temperatures near or below T_g (as for example stated in ISO 815-2) may not be necessary, unless secondary low temperature effects such as crystallization are to be

investigated at the same time.

3.3 Compression set master curves

Since the compression set in the studied materials has a clear viscoelastic origin at low and moderate temperatures, and the neighbouring time segments have similar shapes and overlap quite well near their edges, the postulate of time and temperature equivalence can be applied to construct compression set master curves. A specific shifting routine was implemented in MATLAB in order to obtain a smooth master curve following the approach suggested in [14]. The following function was minimized with respect to the horizontal shifting parameter $a(T)$ for each isothermal time segment being shifted:

$$err = \frac{1}{n}\sum_{i=1}^{n}\frac{\left(y_i(t_i) - \overline{y}_i\left(a(T), t_i\right)\right)^2}{\left(y_i(t_i)\right)^2}$$

Here y_i are the experimental values of the compression set at times t_i, $\overline{y}_i$ are the values of the compression set function approximated by a polynomial, and n is the number measurement points in each time segment. Since the machine unloading time is finite and affects the measurements at short times, the initial period of 100 sec in each segment was ignored. The obtained master curves are presented in Figure 9.

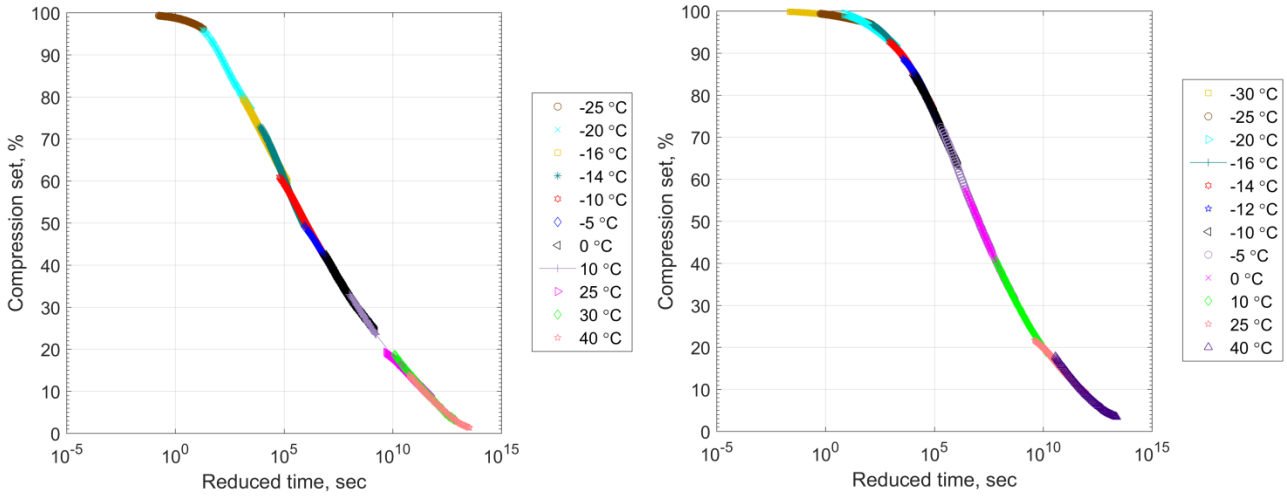

a) unfilled HNBR b) filled HNBR

Figure 9. Master curves of the compression set property of the studied HNBR compounds with T_{ref} = -20 °C. No correction for thermal shrinkage (vertical shifting) was applied

A plot of the shifting factors versus temperature is presented in Figure 10. The figure also demonstrates that the relation between the horizontal shifting factors and temperature can be well described by the WLF equation expressed as [15, 16]

$$\log_{10}(a_T) = \frac{-C_1\left(T - T_{ref}\right)}{C_2 + T - T_{ref}} \quad .$$

It is evident that the carbon black does not have much influence on the temperature variation of the

shifting factor, and the discrepancy between the curves for the filled and unfilled HNBR is probably within the experimental and computing errors in shifting and model fitting. It is also interesting to note that the values of the WLF parameters obtained in both compounds are similar to the "universal" constants for polymers (C_1 = 17.44 and C_2 = 51.6 K) reported in [15].

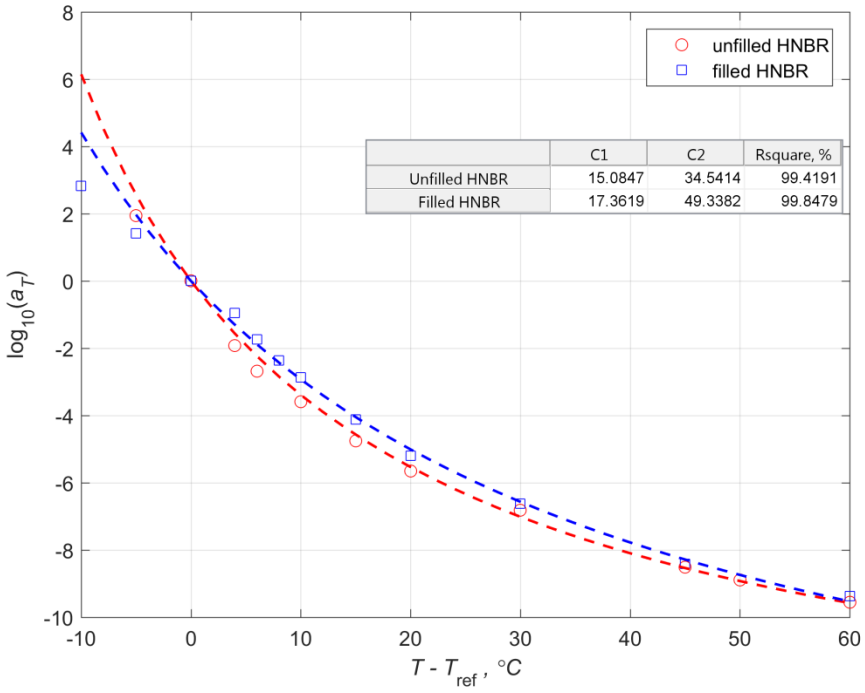

Figure 10. Horizontal shift factor as function of temperature at T_{ref} = -20 °C. The dashed lines represent WLF fit made in the range of -20 to +40 °C.

4. Modelling of the recovery experiment

4.1 Viscoelastic modelling

The recovery after compression should be a viscoelastic process and it should be possible to model the recovery based on the viscoelastic characteristics of the rubber materials. The modelling approach presented here is based on the linear viscoelasticity principles and inspired by [17]. We begin with the Boltzmann superposition principle which yields the following equation for creep strain at time t [16, 17]:

$$\varepsilon(t) = \int_{-\infty}^{t} D(t-u)\frac{d\sigma(u)}{du}du, \tag{1}$$

where $D(t)$ is the creep compliance and $\sigma(t)$ is the stress acting on the material. Since ε and σ are defined from t = 0 the integral can be rewritten to get

$$\varepsilon(t) = \frac{\sigma}{E_0} + \int_{0}^{t} D(t-u)\frac{d\sigma(u)}{du}du \tag{2}$$

Here E_0 is the instantaneous modulus corresponding to the initial elastic response. The compression set test is basically carried out in 2 phases: compression (stress relaxation) phase with duration t_c with no changes in strain and the recovery phase when the load is removed (σ = 0). We also assume

that the initial compression strain ε_0 is known and constant and the unloading step is momentary. Therefore the expression is changed to

$$\varepsilon(t) = \varepsilon_0 + \int_{t_c}^{t} D(t-u)\frac{d\sigma(u)}{du}du \tag{3}$$

Integration by parts knowing $\sigma(t)_{t>t_c} = 0$ gives

$$\varepsilon(t) = \varepsilon_0 - \sigma(t_c)D(t-t_c) \tag{4}$$

It is quite common that the mechanical response of a viscoelastic solid material is successfully modelled by phenomenological approaches using elastic springs and dashpots in series or parallel. To model a stress relaxation process, the generalized Maxwell model consisting of an elastic spring representing equilibrium (long-term) response and *m* Maxwell elements is typically used [16, 18]:

$$\sigma(t) = \varepsilon_0\left[E_\infty + \sum_{i=1}^{m} E_i e^{-(t/\rho_i)}\right], \tag{5}$$

where E_∞ is the equilibrium elastic modulus, E_i are the relaxation strengths and ρ_i are the corresponding relaxation times. The series expression for the Maxwell elements is described mathematically as a Prony series [18]. Although equation (5) is strictly valid only for small strain linear viscoelasticity problems, it is found to approximate the rubber relaxation behaviour relatively well for the moderate strains (up to 15%) used in the compression set experiments reported here. The creep compliance of a viscoelastic solid material is often modelled by the generalized Voigt model with *n* Voigt elements having the following expression [16, 18]:

$$D(t) = D_g + \sum_{j=1}^{n} D_j(1-e^{-(t/\tau_j)}) \tag{6}$$

where D_j are the retardation strengths and τ_j are the corresponding retardation times. D_g is the glassy compliance found by

$$D_g = \frac{1}{E_\infty + \sum_{i=1}^{m} E_i} \tag{7}$$

Incorporating (5) and (6) into (4) one may arrive at

$$\varepsilon(t) = \varepsilon_0\left(1-\left(E_\infty + \sum_{i=1}^{m} E_i e^{-(t_c/\rho_i)}\right)\left[D_g + \sum_{j=1}^{n} D_i\left(1-e^{-\left(\frac{t-t_c}{\tau_i}\right)}\right)\right]_{t\geq t_c}\right) \tag{8}$$

The expression consists of two terms in the parentheses. The first of which accounts for the compression stress relaxation history while the second determines the actual recovery behaviour. Despite a potentially large number of material parameters in the Prony series coming into the formula, it can be easily programmed to supply any number of the Prony elements. After computing the strain recovery, the compression set or the recovery coefficient are calculated in accordance with

the equations in Table 2. A permanent strain term could be added if justified by the experimental data, however this was not considered necessary in this work.

If the recovery test is performed at a temperature T different from the ambient T_c, then the recovery term in the equation has to be evaluated at the temperature of interest. This can be achieved using a physical test or using TTS by shifting the whole retardation spectrum along the time scale by the superposition factor $a_T(T)$ if there is an established and proven relation between a_T and temperature. The equation for the strain recovery at an arbitrary temperature T is, thus, generalized to

$$\varepsilon(t,T) = \varepsilon_0 \left(1 - \left(E_\infty + \sum_{i=1}^{m} E_i e^{-(t_c/\rho_i)} \right) \left[D_g + \sum_{j=1}^{n} D_i \left(1 - e^{-\left(\frac{t-t_c}{a_T(T)\tau_i} \right)} \right) \right]_{t \geq t_c} \right) \tag{9}$$

In practice, it is rather common that only a relaxation or retardation spectrum is available, and therefore a conversion method that is favourable to the user has to be employed. The numerical method proposed by Park and Schapery [19] was used in this work due to its straightforward implementation in MATLAB.

The test data used were quasi-static compression stress relaxation (CSR) master curves measured for these materials [20, 21]. The data were fitted to equation (5) using the sign control method [22] (SCM). An example showing the relaxation data, the fit curves and the obtained relaxation spectra are depicted in Figure 11. It should be noted that the carbon black filled HNBR exhibits higher relaxation strengths in its relaxation spectrum at intermediate and long times if compared to the relaxation spectrum of the unfilled rubber at the same temperature. This effect determines the higher relaxing component of stress and higher CS values observed in the filled rubber during the recovery experiments at temperatures above T_g.

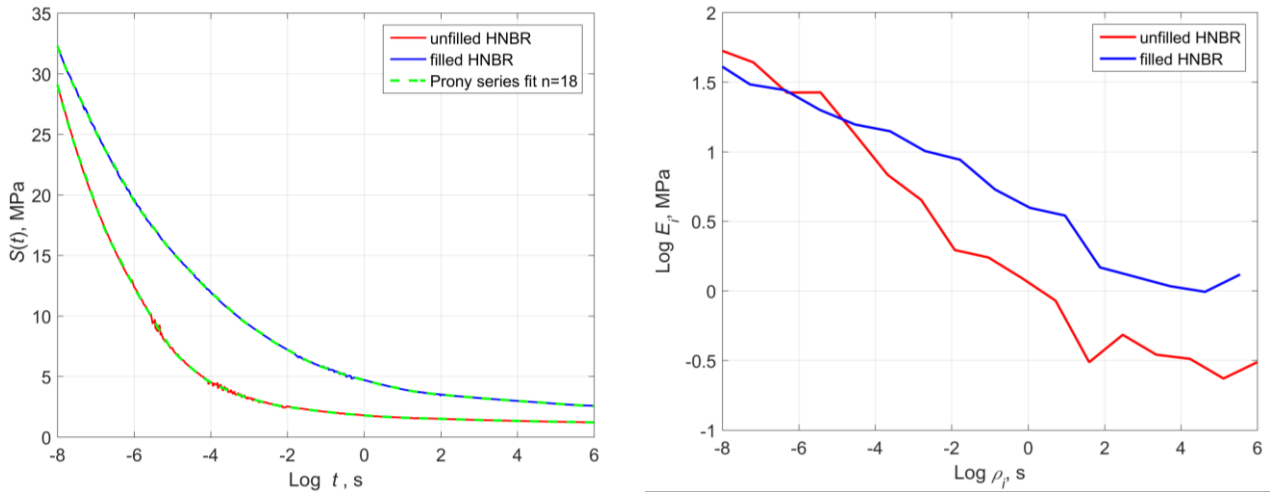

a) b)

Figure 11. a) CSR master curves (solid lines) with T_{ref} = +25 °C [20, 21] and their fitting (dashed lines) by SCM; b) the computed relaxation spectra of the studied HNBR compounds

The full procedure for compression set calculation is illustrated in Figure 12. A comparison of the predictions using this model with experimental data will be discussed below and is shown in Figure 15 and Figure 16.

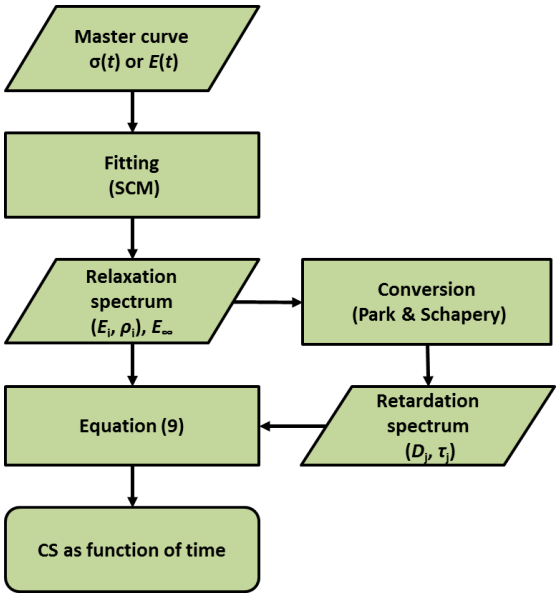

Figure 12. Compression set computation workflow

4.2 FEA modelling

An alternative way to model the shape recovery of the rubber specimens with time is to use finite element analysis (FEA) using the viscoelastic data of the HNBR rubber system. Generally, finite element analysis is a preferable way to determine the behaviour of industrial seals, as they might have intricate cross section geometries and various inserted elements. In this work, Abaqus software (v. 6.14) was used to simulate the performed compression set experiments and verify the proposed model. The FEA model of a cylindrical rubber block compressed by rigid surfaces was made in the axisymmetric setting using CAX4RH linear hybrid elements. The friction coefficient for the rubber block and the mating rigid surfaces was set to 0.2, although this value was found not to significantly affect the results.

The FEA material model consists of two parts: the first is to model the hyperelastic behaviour and the second is for the viscoelastic behaviour with the temperature relation of the superposition factor provided by the WLF equation. The neo-hookean form of the strain energy density function was chosen as a hyperelastic material model for the FEA since only moderate strains are of concern in the current investigation. The strain energy density function for a compressible neo-hookean material is typically formed of the deviatoric and the volumetric terms [23, 24] and expressed as:

$$W = C_{10}\left(\bar{I}_1 - 1\right) + D_1\left(J - 1\right)^2$$

where C_{10} and D_1 are material parameters representing the resistance to shear and the

compressibility of the material respectively; $\bar{I}_1 = J^{-2/3} I_1$ is the the first deviatoric strain invariant; $J = \lambda_1 \lambda_2 \lambda_3$ and $I_1 = \lambda_1^2 + \lambda_2^2 + \lambda_3^2$ is the first strain invariant expressed in terms of the principal stretch ratios λ_i. The parameter C_{10} is found from fitting of the corresponding long-term compression stress-stretch data demonstrated in Figure 13, while the compressibility was measured earlier [9]. The model adequately fits the uniaxial compression data sets for both compounds yielding only a slightly higher fitting error than the models with larger number of material parameters [21].

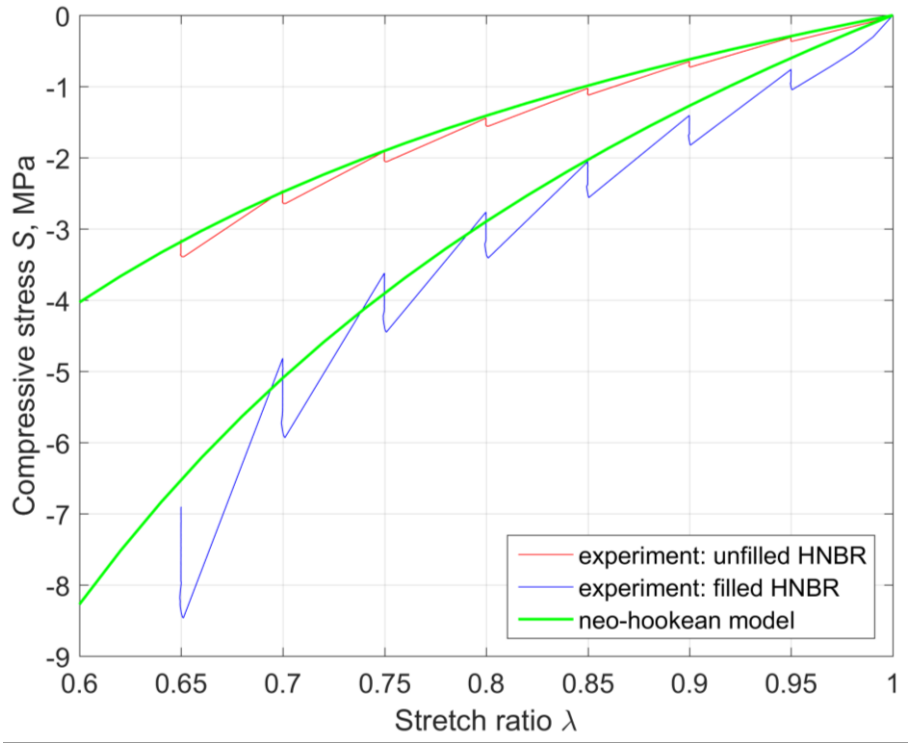

Figure 13. Step strain CSR response at +40 °C as function of stretch ratio and fitting of the relaxed (long-term) stress data by the neo-hookean model. Cylindrical specimens were compressed in the Eplexor machine using the same compression holder. A silicone grease was applied to minimise barrelling. The strain rate here is approximately 0.005 sec^{-1}. The strain step length is 0.05, and linear interpolation is used between the measurement points.

The material model parameters used in the FEA are listed in Table 3.

Table 3 Long-term material properties used in FEA

Parameter	Unfilled HNBR	Carbon black filled HNBR
C_{10} , MPa	0.92	1.89
D_1 , MPa^{-1}	0.001	0.00087

The viscoelastic material behaviour is modelled by the Prony series in dimensionless form as required by Abaqus. The same CSR data sets were used to identify the viscoelastic material parameters for the FEA. The number of Prony series terms was, however, reduced to 13 to comply

with the limitation of the software.

An example of the visualization output of the performed FEA is shown in Figure 14.

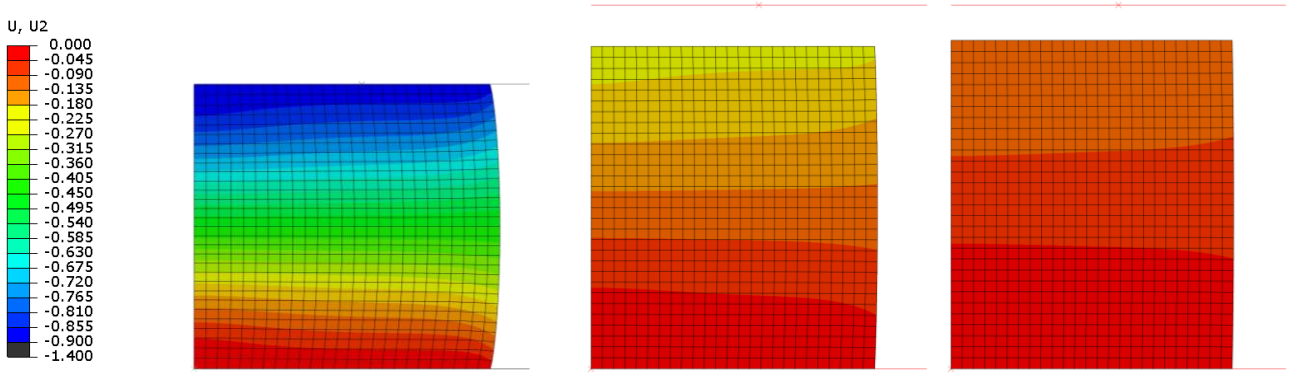

0 sec 5 sec 200 sec

Figure 14. Images of the simulated compression set test at the ambient temperature. The times indicated are after the load is released.

4.3 Comparison with experimental data

The experimental CS data for the unfilled HNBR and filled HNBR are plotted in Figure 15 and Figure 16 respectively together with the modelling results.

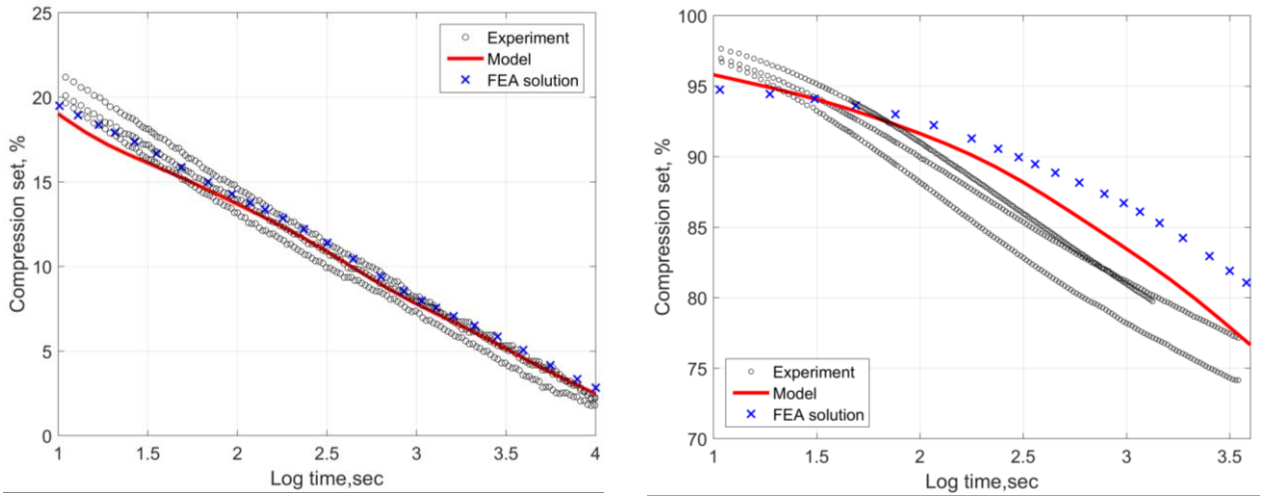

a) +25 °C b) -20 °C

Figure 15. Experimental and modelling results of the compression set as function of time for the unfilled HNBR at a) 25 °C and b) -20 °C. The data in b) are corrected for the thermal contraction.

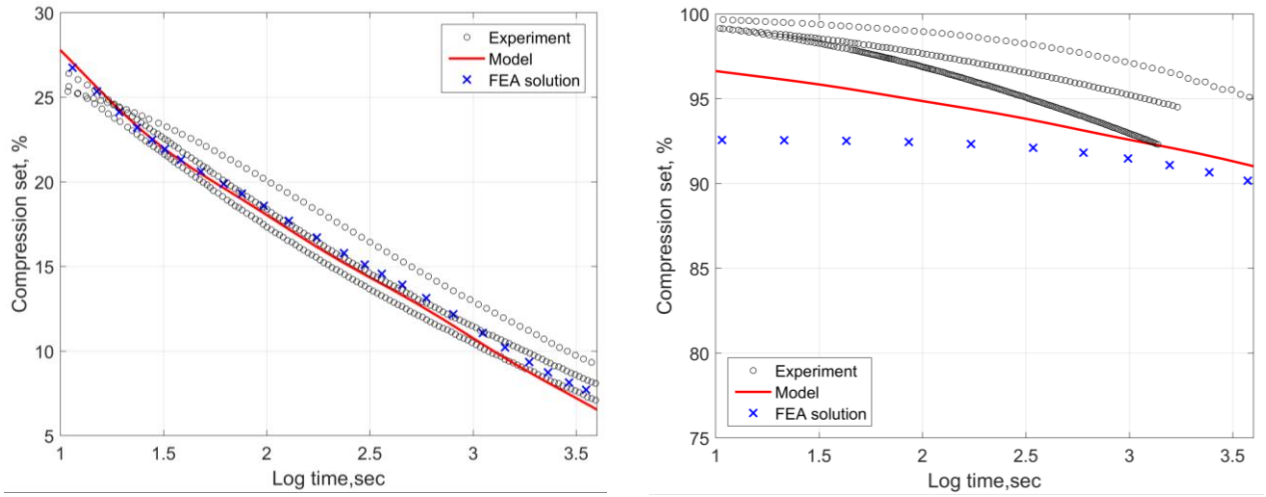

a) +25 °C b) -20 °C

Figure 16. Experimental and modelling results of the compression set as function of time for the carbon black filled HNBR at a) 25 °C and b) -20 °C. The data in b) are corrected for the thermal contraction.

Both models predict the elastic recovery of HNBR quite well at ambient temperature (+25 °C) and acceptably at around the glass transition temperature (-20 °C). The deviation between the FEA solution and the proposed model is rather small and presumably related to the difference in fitting of the relaxation data and the limited number of the Prony elements in Abaqus as described above. Another potential source of this small discrepancy is the necessary use of the hyperelastic material model in FEA dictated by the finite strains in the model.

The largest differences between the experiment and modelling results of about 5 % are observed close to T_g in both compounds. In general, the thermo-mechanical behaviour of rubber becomes more complex in the vicinity of T_g, and there can be several reasons for the noticeable deviation. The first potential explanation is the known temperature dependency of the rubber modulus which has not been not accounted for in the modelling approach (it directly affects the compression history term). Therefore, for more accurate results in the case of large temperature differences a correction factor, e.g. a vertical shifting factor $b_T(T)$, should be introduced. Furthermore, the cooling (or heating) process takes time during which some incomplete relaxation processes may still take place at rates varying with the temperature. This effect is, however, not considerable at T_g as evident from the experiments with varying initial compression times (Figure 8b).

The mechanical behaviour of rubber at finite strains in the glassy state or on the upper shelf of the transition region might no longer be correctly described by the simple models used in this work. As such, both FE and analytical approaches might fail to give accurate estimates of CS below T_g. Nonetheless, as demonstrated by this work and many other experiments [3, 4, 6-8], rubber at these temperatures exhibits no or very limited recovery manifested in CS values of about 100 %.

The modelling approach could also be extended to predict CS in rubber exposed to elevated temperatures. The necessary condition for the utilization is that the stress relaxation at these

temperatures is governed only by physical mechanisms and that there is a complete relaxation data set (a relaxation or retardation spectrum) available at short and long times. If the physical relaxation is augmented with some chemical relaxation processes, the approach will most likely stop yielding adequate estimates of CS. The variation of the horizontal shifting factor with temperature, if used, should be well characterized since low accuracy in its temperature relation might also be a significant source of error in the CS estimation.

The modelling approach can also help explain the noticeable difference in CS values demonstrated in Figure 8 when the initial compression is applied with various durations. In the case of a short compression relaxation period (the relaxation processes in the rubber are incomplete) the compression history term in equation (9) is high and facilitates the strain recovery to proceed much faster. If the compression relaxation time is much longer, the contribution of the compression history term decreases, approaching the equilibrium state at long times (E_∞) and, thus, the computed recovery rate is much smaller and in accordance with the experimental observations. In contrast to the ambient conditions, the CSR term becomes negligible at, and below, T_g in comparison with the recovery term at the same temperature. Hence, the recovery rate is mostly governed by the retardation spectrum at these temperatures.

5. Conclusions

The following conclusions can be drawn based on the experimental results and the subsequent modelling:

1. The studied HNBR compounds (with and without the addition of 50 phr carbon black) possess rather poor recovery at low temperatures at and near the glass transition region demonstrated by large compression set (CS) values of 70-100 % at these temperatures. Nevertheless, the compression set might approach zero even at low temperatures near T_g provided there is substantial time for the shape recovery;
2. The duration of the initial compression has a significant effect on the elastic recovery in the CS experiments conducted at ambient temperature, while the effect becomes minimal at sub-zero conditions once the glass transition region is reached;
3. Carbon black as a filler imparts inferior low temperature recovery properties to HNBR compared to the unfilled HNBR, although the negative effect is not substantial at ambient conditions. The largest difference of about 20 % between the property values in the filled and unfilled HNBR is observed near the T_g region. Below this temperature both compounds demonstrate no or minimal elastic recovery;
4. The time-temperature superposition principle is found to be applicable to the HNBR compression set data measured at various temperatures, since the neighbouring isothermal time segments overlap quite well. The variation of the horizontal shifting parameter a_T with temperature is well fitted by the WLF expression with the parameters being similar to the

"universal" values for polymers regardless of if the HNBR compound is reinforced or not.

5. A viscoelastic model for prediction of the time variation of the strain recovery is proposed. The model links the basic relaxation characteristics of a rubbery material, such as the relaxation spectrum obtained from stress relaxation experiments, with the compression set in the material. It is demonstrated that the model prediction matches the FEA modelling output and it successfully captures the recovery behaviour of the studied HNBR at ambient temperature.
6. The modelling approach can also be used to predict rubber recovery at low and moderately elevated temperatures provided that only physical relaxation processes occur in the studied material and the temperature relation of time-temperature superposition factor a_T is available.

6. Declaration of interest

The authors declare that they have no conflict of interest.

7. Acknowledgments

This work is part of the collaborative project "Thermo Responsive Elastomer Composites for cold climate application" with the industrial partners FMC Kongsberg Subsea AS, STATOIL Petroleum AS, The Norwegian University of Science and Technology (NTNU) and the research institute SINTEF Materials and Chemistry. The authors would like to express their thanks for the financial support by The Research Council of Norway (Project 234115 in the Petromaks2 programme).

References

[1] B.N.J. Persson, O. Albohr, U. Tartaglino, A.I. Volokitin, E. Tosatti, On the nature of surface roughness with application to contact mechanics, sealing, rubber friction and adhesion, Journal of Physics: Condensed Matter 17(1) (2005) R1.

[2] R.E. Morris, J.W. Hollister, P.A. Mallard, The Cold-Compression sets of Natural and Synthetic Vulcanizates, Rubber Chem Technol 19(1) (1946) 151-162.

[3] B.M. Gorelik, M.F. Bukhina, Effect of degree of compression of rubber on strain recovery and contact pressure (in Russian) Kauchuk i Rezina (9) (1961) 22-26.

[4] B.M. Gorelik, M.F. Bukhina, Crystallization of rubber at low temperatures in compression (in Russian), Kauchuk i Rezina (11) (1961) 11-15.

[5] N.S. Baranov, A.I. El'kin, Loss of resilience of rubber seals at low temperatures (in Russian), Kauchuk i Rezina (5) (1974) 33-37.

[6] M.F. Bukhina, M.D. Parizenberg, Temperature-Strain Superposition of Elastomer Properties near the Transition from Rubberlike into Glassy State (in Russian), Vysokomol Soedin B 23(6) (1981) 456-460.

[7] M. Jaunich, W. Stark, D. Wolff, A new method to evaluate the low temperature function of rubber sealing materials, Polymer Testing 29(7) (2010) 815-823.

[8] M. Jaunich, W. Stark, D. Wolff, Comparison of low temperature properties of different elastomer materials investigated by a new method for compression set measurement, Polymer Testing 31(8) (2012)

987-992.
[9] A.G. Akulichev, B. Alcock, A. Tiwari, A.T. Echtermeyer, Thermomechanical properties of zirconium tungstate/hydrogenated nitrile butadiene rubber (HNBR) composites for low-temperature applications, J Mater Sci 51(24) (2016) 10714-10726.
[10] ISO 815-2: Rubber, vulcanized or thermoplastic - Determination of compression set - Part 2: At low temperatures, The International Organization for Standardization, 2008.
[11] GOST 13808-79. Method for determination of low temperature resistance according to elastic rebound after compression, Standards Publisher, Moscow, 1988.
[12] G. Kraus, Reinforcement of elastomers by carbon black, Rubber Chem Technol 51(2) (1978) 297-321.
[13] J.L. Leblanc, Filled polymers : science and industrial applications, CRC Press, Boca Raton, 2010.
[14] J. Honerkamp, J. Weese, A note on estimating mastercurves, Rheol Acta 32(1) (1993) 57-64.
[15] M.L. Williams, R.F. Landel, J.D. Ferry, Mechanical Properties of Substances of High Molecular Weight .19. The Temperature Dependence of Relaxation Mechanisms in Amorphous Polymers and Other Glass-Forming Liquids, J Am Chem Soc 77(14) (1955) 3701-3707.
[16] J.D. Ferry, Viscoelastic properties of polymers, Wiley, New York, 1980.
[17] C. Joubert, A. Michel, L. Choplin, P. Cassagnau, Influence of the crosslink network structure on stress-relaxation behavior: Viscoelastic modeling of the compression set experiment, Journal of Polymer Science Part B: Polymer Physics 41(15) (2003) 1779-1790.
[18] N.W. Tschoegl, The phenomenological theory of linear viscoelastic behavior : an introduction, Springer-Verlag, Berlin ; New York, 1989.
[19] S.W. Park, R.A. Schapery, Methods of interconversion between linear viscoelastic material functions. Part I—a numerical method based on Prony series, Int J Solids Struct 36(11) (1999) 1653-1675.
[20] A.G. Akulichev, A. Echtermeyer, B. Alcock, Stress relaxation in HNBR at low temperatures, The International Rubber Conference 2016 (IRC2016), Kitakyushu, Japan, 2016.
[21] A. Akulichev, A. Echtermeyer, B. Alcock, Compression stress relaxation in carbon black reinforced HNBR at low temperatures. To be published.
[22] R.D. Bradshaw, L.C. Brinson, A Sign Control Method for Fitting and Interconverting Material Functions for Linearly Viscoelastic Solids, Mech Time-Depend Mat 1(1) (1997) 85-108.
[23] O.H. Yeoh, Developments in Finite Element Analysis, Engineering with Rubber, Carl Hanser Verlag GmbH & Co. KG2012, pp. 345-364.
[24] Abaqus/CAE user's guide. Ver. 6.14, Dassault Systèmes, Providence, RI, 2014.